Momentum Dependent Spectral Changes Induced by the Charge Density Wave in $2H$-$TaSe_2$ and the Implication on the CDW Mechanism

Rong Liu,[1] C. G. Olson,[2] W. C. Tonjes,[1] and R. F. Frindt[3]
[1]*Department of Physics and Astronomy, Michigan State University, East Lansing, Michigan 48824*
[2]*Ames Laboratory, Ames, Iowa 50011*
[3]*Department of Physics, Simon Fraser University, Burnaby, British Columbia, Canada V5A 1S6*
(Received 25 August 1997; revised manuscript received 4 December 1997)

We report a high energy and high angular resolution angle resolved photoemission study of $2H$-$TaSe_2$ at temperatures both above and below the charge-density-wave (CDW) transition. In the normal state, an extended saddle band very close to the Fermi energy was observed. The CDW-induced energy gap is near zero on a well defined Fermi surface and large in the extended saddle band region. The implication of these results on the CDW mechanism is discussed. [S0031-9007(98)06472-2]

PACS numbers: 71.45.Lr, 79.60.Bm

Many layered transition-metal dichalcogenides, in their various polytypes, exhibit a range of charge-density-wave (CDW) transitions. The structural and transport properties associated with the CDW have been well studied [1]. In general, compounds with the $1T$ structure, such as $1T$-TaS_2, have a strong first order CDW transition. The in-plane resistivity increases in the CDW state. On the other hand, compounds with the $2H$ structure, such as $2H$-$TaSe_2$, have a weak second order CDW transition. The in-plane resistivity decreases in the CDW state.

$2H$-$TaSe_2$ undergoes an incommensurate CDW transition at 122 K, followed by a commensurate CDW transition at 90 K [1]. In the commensurate CDW state, the material has a 3×3 superlattice aligned along the same axes as the unreconstructed 1×1 lattice. $2H$-$TaSe_2$ is one of the first materials to be studied by angle resolved photoemission (ARPES) [2]. The energy resolution was rather poor at that time and the measurements were usually made at room temperature. In recent years, the energy and angular resolutions have gradually improved and cryogenic temperatures can be achieved. Smith *et al.* [3] first carried out ARPES studies of $2H$-$TaSe_2$ in the presence of CDW. The CDW-induced energy gap near the Fermi energy (E_F) was not investigated, probably due to insufficient energy resolution. More recently, Dardel *et al.* [4] performed ARPES measurements of $2H$-$TaSe_2$ using a high energy resolution ($\Delta E = 20$ meV) but moderate angular resolution ($\pm 3°$) spectrometer. They measured the spectra at two emission angles along the Γ-K direction above and below the CDW transition temperature, and found that the CDW-induced spectral changes near E_F are very different at these two angles. Because of their limited angular resolution, the detailed angular dependence of the energy gap was not determined. ARPES studies of the CDW-induced spectral changes in the quasi-one-dimensional blue bronzes ($K_{0.3}MoO_3$ and $Rb_{0.3}MoO_3$) and $(TaSe_4)_2I$ have been reported by Dardel *et al.* [5] and Terrasi *et al.* [6], respectively.

In this Letter, we report a high energy and high angular resolution ($\Delta E = 30$ meV, $\Delta\theta = \pm 1°$) ARPES study of $2H$-$TaSe_2$. In the normal state, we observed an extended saddle band along Γ-K. This band is nearly flat and very close to E_F, much closer than what band theory predicts. A well defined Fermi surface was observed near the Γ point. Another Fermi surface, although somewhat ambiguous, was also observed near the K point. In the CDW state, the energy gap is found to be near zero on the well defined Fermi surface and large in the extended saddle band region.

Single crystal samples of $2H$-$TaSe_2$ were grown using the iodine-vapor transport method. ARPES measurements were carried out at the Ames-Montana ERG-Seya beam line at the Synchrotron Radiation Center, in Stoughton, Wisconsin. A movable 50-mm-radius hemispherical electron energy analyzer was used. The combined (electron and photon) energy resolution of the photoelectron spectrometer was 30 meV at 1.5 eV pass energy and 21 eV photon energy. The angular resolution of the electron analyzer was $\pm 1°$, which corresponds to a momentum resolution of 0.073 $Å^{-1}$ for measurements near the Fermi level using 21 eV photons. Single crystal samples were oriented using x-ray Laue diffraction prior to mounting in the chamber. Clean surfaces were obtained by cleaving the sample in a vacuum better than 3×10^{-11} Torr. Samples were cooled to 20 K using a closed cycle helium refrigerator. A resistor heater was used to heat the sample above the CDW transition temperatures. Fermi level reference was obtained on a clean platinum foil which was in electrical contact with the sample.

Figure 1 shows the energy distribution curves (EDC's) in the normal state ($T = 125$ K) for k points along three lines in the Brillouin zone. Figure 1(a) is for k along Γ-K; Figs. 1(b) and 1(c) are for k along two lines parallel to but slightly away from Γ-K (see the inset of Fig. 1). The k_x and k_y values marked along each curve, in $Å^{-1}$, are momentum components parallel and perpendicular to Γ-K, respectively. The Γ and K points are at $(k_x, k_y) = (0, 0)$ and $(1.22, 0)$, respectively. All spectra were normalized to photon flux. In Fig. 1(a), there is very little spectral intensity at E_F at $(k_x, k_y) = (0.36, 0)$ (bottom curve). [The EDC's for (k_x, k_y) before $(0.36, 0)$ (not shown) all

 0031-9007/98/80(26)/5762(4)$15.00

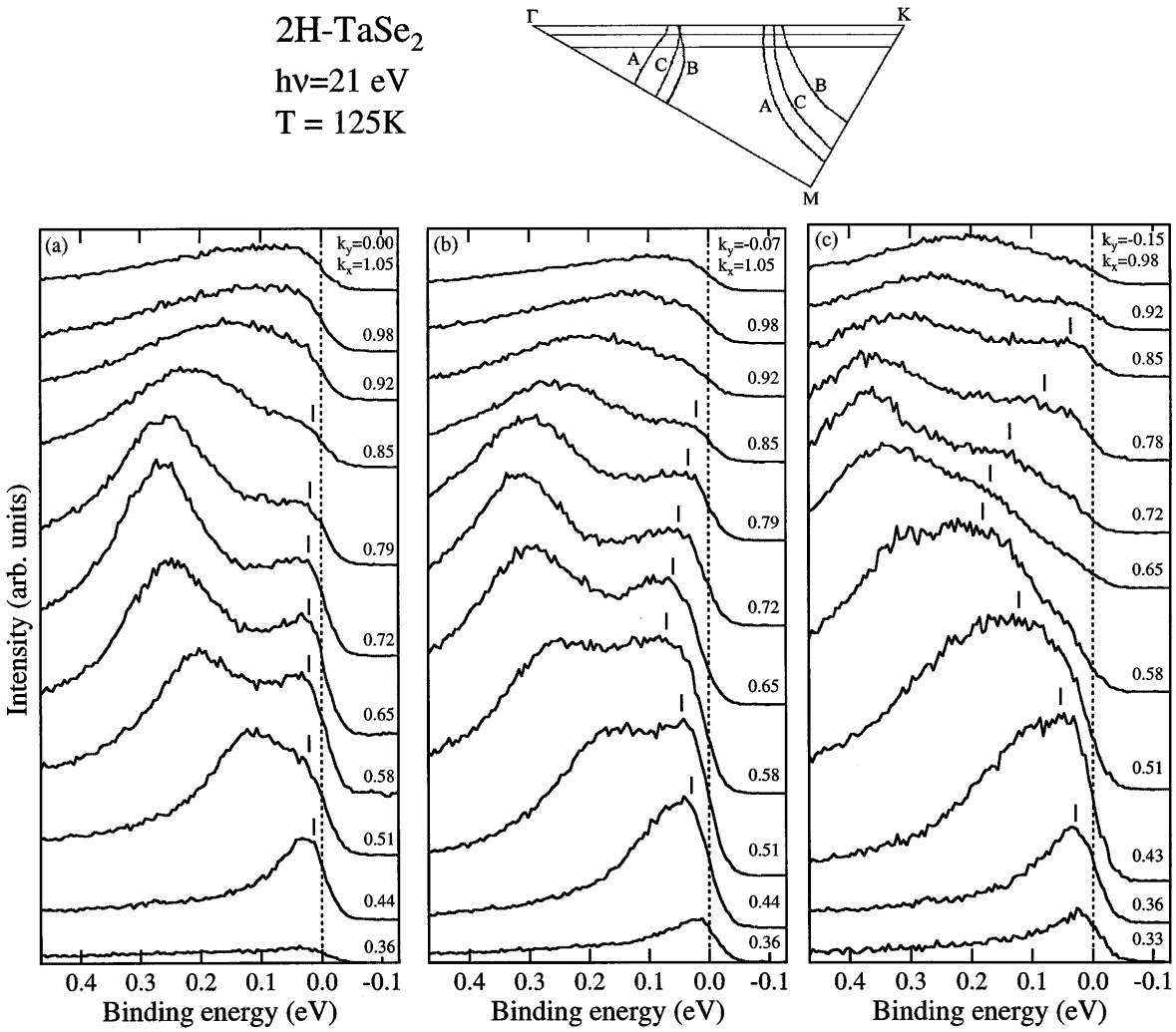

FIG. 1. Energy distribution curves (EDC's) in the normal state ($T = 125$ K), for k points along three lines in the Brillouin zone: (a) along Γ-K; (b) and (c) along two lines parallel to but slightly away from Γ-K. The k_x and k_y values marked along each curve, in Å^{-1}, are momentum components parallel and perpendicular to Γ-K, respectively. The Γ and K points are at $(k_x, k_y) = (0, 0)$ and $(1.22, 0)$, respectively. All spectra are normalized to photon flux. The inset (top) shows the irreducible wedge of the Brillouin zone with the Fermi surfaces predicted by band calculations [7]. (A: $k_z = 0$; B: $k_z = 2\pi/c$; C: $k_z = \pi/c$. The separations between them indicate the amount of k_z dispersion.) The three lines corresponding to the k points in (a), (b), and (c) are also indicated.

have very low intensities at E_F.] When (k_x, k_y) is changed to $(0.44, 0)$, a strong quasiparticle peak appears at E_F, suggesting that a band has moved from above E_F to below E_F at this point. Thus, $(k_x, k_y) = (0.44, 0)$ is a point on the Fermi surface. As k is further increased, the peak splits into two peaks. One disperses to a maximum binding energy of about 0.25 eV before dispersing back toward E_F; the other stays close to E_F for an extended region, as indicated by the vertical dashes (the dashes are placed at the apparent peak positions, which are not the true binding energies, as will be explained below). Note that the latter is extremely close to E_F and very narrow since the Fermi level (the vertical dashed line) lies above the midpoints of the leading edges. When a peak is close to E_F, the apparent peak position is not the true binding energy due to the effect of the finite resolution function. When (k_x, k_y) is changed from $(0.79, 0)$ to $(0.85, 0)$, the spectral feature near E_F becomes broader and its line shape changes from a peak to a shoulder, suggesting that the band may have crossed E_F at $(k_x, k_y) = (0.85, 0)$. This Fermi crossing, however, is not as well defined as the first Fermi crossing, since there are still substantial spectral intensities near E_F beyond $(k_x, k_y) = (0.85, 0)$. The flat band probably remains near E_F.

In Figs. 1(b) and 1(c), we see a similar general trend. Well defined Fermi crossings can be observed at $(k_x, k_y) = (0.36, -0.07)$ and $(0.33, -0.15)$ in Figs. 1(b) and 1(c), respectively. These Fermi crossings, along with the one at $(k_x, k_y) = (0.44, 0)$, form a Fermi surface locus centered on the Γ point. Note that, in Fig. 1(b), the near E_F band disperses significantly below E_F in the midrange, as indicated by the vertical dashes. As the band disperses back toward E_F, it appears to cross E_F at $(k_x, k_y) = (0.85, -0.07)$. In Fig. 1(c) where k points are along a line

further away from Γ-K, the band disperses even further below E_F in the midrange, and appears to cross E_F at $(k_x, k_y) = (0.85, -0.15)$. The second Fermi crossings in Figs. 1(b) and 1(c) are more obvious than the one in Fig. 1(a) because the band has a finite dispersion. The fact that this band stays close to E_F for an extended region along Γ-K and disperses below E_F in the direction perpendicular to Γ-K in the midrange suggests that it is an *extended saddle band.*

Shown in the inset of Fig. 1(top) is the irreducible wedge of the Brillouin zone along with the Fermi surfaces calculated by Wexler and Woolley [7]. (The lines labeled *A*, *B*, and *C* correspond to the Fermi surfaces for $k_z = 0, 2\pi/c, \pi/c$, respectively. The separations between them indicate the predicted amount of k_z dispersion.) The observed Fermi crossings are in good accord with the calculations.

Figure 2 shows the EDC's in the commensurate CDW state ($T = 20$ K) for the same set of k points along Γ-K as in Fig. 1(a) (in terms of the unreconstructed 1×1 Brillouin zone). Again, the spectra were normalized to photon flux. For comparison, the EDC's in the normal state ($T = 125$ K) were superimposed as the dashed curves. It can be seen that the CDW-induced spectral changes are highly k dependent. At $(k_x, k_y) = (0.44, 0)$, which is a Fermi surface crossing point, the change near E_F is relatively small. The leading edge is slightly sharper at low temperature, which can be accounted for by the reduced thermal broadening. The Fermi level remains above the midpoint of the leading edge, indicating that the CDW-induced energy gap is very small or near zero. For (k_x, k_y) beyond $(0.44, 0)$, the spectral changes are much more dramatic. Note that the leading edges shift significantly toward higher binding energies at low temperature, indicating the removal of electronic states from the Fermi level.

During the experiment, measurements were repeated several times as the sample went through temperature cycles between 20 and 125 K. The spectra were reproducible and no surface degradation was detected. Measurements with small temperature increments between 20 and 125 K showed that the spectral change is correlated with the CDW transition. As the sample temperature was changed from 20 to 125 K, the thermal expansion of the sample holder (made of copper) was approximately 0.2 mm. The photon spot was about 0.6 mm in diameter. Measurements were made both with and without the sample height adjusted to compensate for the thermal expansion. The spectra were qualitatively similar but did show some intensity difference, part of which may be due to sample inhomogeneities, part of which may be due to slightly different alignment.

To quantify the momentum dependence of the energy gap, we estimate the energy shift between the leading edge midpoints in the normal and CDW state. Different methods of determining the gap might change the numbers slightly, but will not change the curve shape. The energy shift as a function of k along Γ-K is plotted in Fig. 3(a).

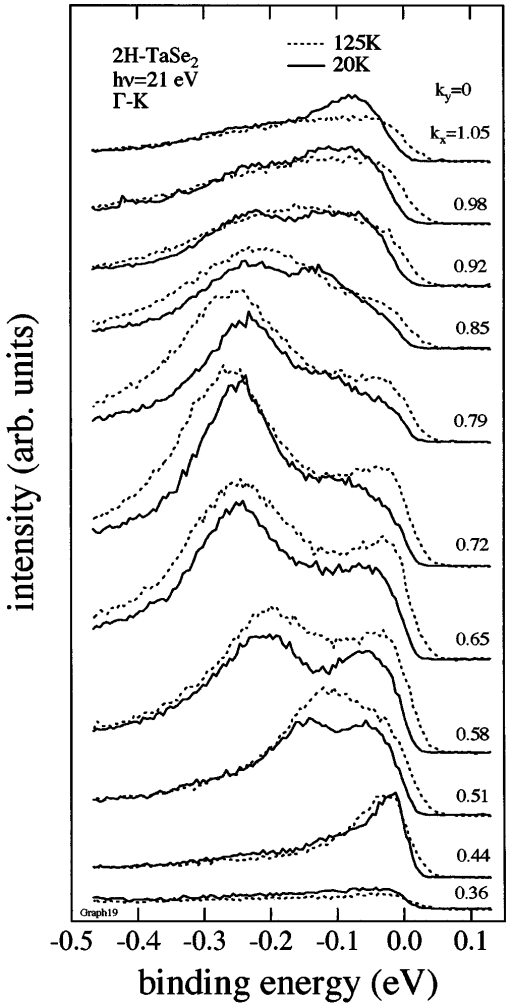

FIG. 2. EDC's in the commensurate CDW state ($T = 20$ K, solid curves), for the same set of k points along Γ-K as in Fig. 1(a) (in terms of the unreconstructed 1×1 Brillouin zone). The EDC's in the normal state are superimposed as the dashed curves for comparison.

Strictly speaking, a gap can be defined only on the Fermi surface. Here, we also use the term "gap" for the extended saddle band region, since there are states near E_F at those k points and they are affected by the CDW formation. As can be seen, the energy shift is near zero at $k = 0.44$ Å^{-1}, which is a Fermi crossing point. It increases to finite values in the extended saddle band region. At larger wave vectors along Γ-K ($k > 1.05$ Å^{-1}), the energy shift remains large (comparable to $k = 1.05$ Å^{-1}), but the spectral intensity at E_F diminishes. Temperature dependent measurements were made at other points on the Fermi surface centered on the Γ point, including a point along Γ-M, the CDW wave vector direction. The energy shifts at those k points are all near zero [8].

Shown in Fig. 3(b) are the band dispersions (solid circles) extracted from the EDC's in Fig. 1(a). The solid lines are the band calculation results by Wexler and Woolley [7]. The calculation predicts two bands near E_F, both derived from the d_{z^2} orbital of the Ta-5d electrons. The

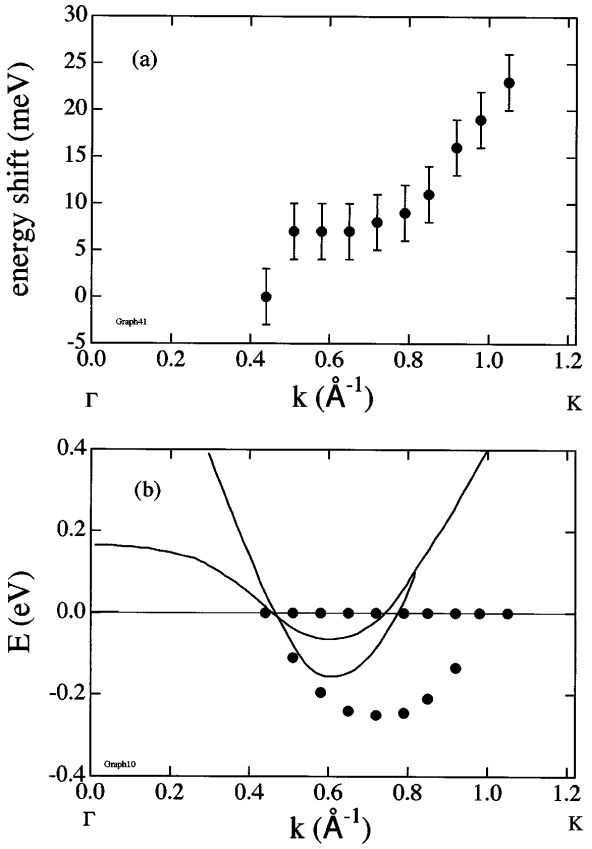

FIG. 3. (a) The energy shift vs k along Γ-K. The energy shift is taken as the binding energy difference of the leading edge midpoints in the normal and CDW state spectra. (b) Normal state band dispersions along Γ-K extracted from the EDC's in Fig. 1(a) (solid circles). The solid lines are the band calculation results by Wexler and Woolley [7].

splitting between the two bands is caused by intersandwich interaction within a unit cell. The two bands are almost degenerate as they cross E_F, once closer to the Γ point, and again closer to the K point, forming the two Fermi surfaces depicted in the inset in Fig. 1. Experimentally, we also observed two bands. However, the dispersion of one band is larger than predicted, and that of the other is much less. We note that Wexler and Woolley used a non-self-consistent and nonrelativistic method in their calculations. It is highly desirable to have a density functional calculation based on full potentials and including spin-orbit coupling. Our data should be compared with such a calculation when it becomes available.

Traditionally, Fermi surface nesting has been considered as the main mechanism for CDW formation. However, the $2H$ polytype transition-metal dichalcogenides are better conductors in the CDW phase [1], indicating that most of the Fermi surface is not affected. Rice and Scott [9] proposed an alternative mechanism which invokes the saddle points on the Fermi surface [10]. In their model, the CDW phase is metallic with only a relatively small area of the Fermi surface truncated at the saddle points. These saddle points act as scattering sinks in the normal state and their removal can lead to an enhancement of the conductivity. The validity of this model was questioned by Wexler and Woolley [7] since their calculations place the saddle point quite far below E_F. As we have shown above, the saddle band is indeed very close to E_F; moreover, the energy gap is large in the saddle band region and small on the other parts of the Fermi surface. Our results suggest that the Rice-Scott model might be relevant. However, we observed an extended saddle band instead of a single saddle point as in the Rice-Scott model. The nesting property of the extended saddle band and its relation to the CDW wave vector are not yet clear and need further investigations.

In summary, we performed high energy and high angular resolution ARPES measurements on $2H$-$TaSe_2$ at temperatures both above and below the CDW transition. In the normal state, we observed an extended saddle band along Γ-K, which lies very close to E_F, much closer than band theory predicts [7]. In the CDW state, the energy gap is found to be large in the extended saddle band region and near zero at other parts of the Fermi surface. We suggest that our data provide possible experimental support for the "saddle-point" CDW mechanism proposed by Rice and Scott [9].

This work is based upon research conducted at the Synchrotron Radiation Center, University of Wisconsin-Madison, which is supported by the NSF under Award No. DMR-95-31009. Ames Laboratory was operated for the U.S. DOE by Iowa State University under Contract No. W-7405-ENG-82. Support of the Natural Sciences and Engineering Research Council of Canada is also acknowledged.

[1] For reviews, see J. A. Wilson, F. J. DiSalvo, and S. Mahajan, Adv. Phys. **24**, 117 (1975); R. V. Coleman *et al.*, Adv. Phys. **37**, 559 (1988).
[2] N. V. Smith and M. M. Traum, Phys. Rev. B **11**, 2087 (1975).
[3] N. V. Smith, S. D. Kevan, and F. J. DiSalvo, J. Phys. C **18**, 3175 (1985).
[4] B. Dardel *et al.*, J. Phys. Condens. Matter **5**, 6111 (1993).
[5] B. Dardel *et al.*, Europhys. Lett. **19**, 525 (1992).
[6] A. Terrasi *et al.*, Phys. Rev. B **52**, 5592 (1995).
[7] G. Wexler and A. M. Woolley, J. Phys. C **9**, 1185 (1976).
[8] R. Liu, W. C. Tonjes, C. G. Olson, and R. F. Frindt (unpublished).
[9] T. M. Rice and G. K. Scott, Phys. Rev. Lett. **35**, 120 (1975).
[10] L. F. Mattheiss, Phys. Rev. B **8**, 3719 (1973).